



Effects of climate change and nutrient concentrations on carbon sources for zooplankton in a Tibetan Plateau lake over the past millennium

Yaling Su · Kuanyi Li · Yongdong Zhang · Zhengwen Liu · Tijian Wang · Erik Jeppesen · Jack J. Middelburg · John P. Smol

Received: 28 October 2021 / Accepted: 1 May 2022 / Published online: 29 May 2022
© The Author(s), under exclusive licence to Springer Nature B.V. 2022

Abstract Autochthonous and allochthonous organic carbon (OC) are important carbon sources for zooplankton in lakes, and changes in the abundance and proportions of those sources may affect zooplankton community composition and lake ecosystem function. Nevertheless, long-term changes in assimilation of autochthonous and allochthonous carbon by zooplankton and associated climate- and environment-related forcing mechanisms have rarely been studied.

We used a sediment record of cladoceran remains and geochemical variables from Lake Jirentso on the Tibetan Plateau to track long-term changes in sources of carbon for cladocera over the past ~950 years. High cladoceran:diatom accumulation rate ratios during the cold Little Ice Age indicated that cladocerans assimilated more allochthonous OC that was released from glaciers and frozen soils to replenish their food supply, a consequence of low primary production in the lake. In contrast, low cladoceran:diatom accumulation rate ratios during the Current Warm Period indicated that cladocerans utilized more autochthonous

Supplementary Information The online version contains supplementary material available at <https://doi.org/10.1007/s10933-022-00245-w>.

Y. Su (✉) · K. Li · Z. Liu
Nanjing Institute of Geography and Limnology,
Chinese Academy of Sciences, 73 East Beijing Road,
Nanjing 210008, China
e-mail: ylsu@niglas.ac.cn

Y. Zhang
School of Geography, South China Normal University,
Guangzhou 510631, China

Z. Liu
Department of Ecology, Jinan University,
Guangzhou 510632, China

Z. Liu · E. Jeppesen
Sino-Danish Centre for Education and Research (SDC),
University of Chinese Academy of Sciences, Beijing,
China

T. Wang
School of Atmospheric Sciences, Nanjing University,
Nanjing 210093, China

E. Jeppesen
Department of Bioscience, Aarhus University, Vejløvej
25, 8600 Silkeborg, Denmark

E. Jeppesen
Limnology Laboratory, Department of Biological Sciences
and Centre for Ecosystem Research and Implementation,
Middle East Technical University, Ankara 60800, Turkey

E. Jeppesen
Institute of Marine Sciences, Middle East Technical
University, Mersin 37731, Turkey

J. J. Middelburg
Department of Earth Sciences, Utrecht University,
Princetonlaan 8A, 3584 CB Utrecht, The Netherlands

J. P. Smol
Paleoecological Environmental Assessment and Research
Lab (PEARL), Department of Biology, Queen's
University, Kingston, ON K7L 3N6, Canada

OC. Less autochthonous OC was available for cladocerans during the Medieval Warm Period than during the Current Warm Period. The total accumulation rate of cladocerans was significantly correlated with the annual mean air temperature, total phosphorus, and the organic carbon to nitrogen ratio in the sediment core. Recent warming and sharply increased nutrient inputs affected the cladoceran and diatom assemblages, further inducing a shift in the diet of zooplankton towards more recently produced OC. The sediment record from Lake Jirentso, which represents the last ~950 years of deposition, spanned an ideal time window for assessing historical changes related to the impacts of climate and nutrients on zooplankton carbon sources.

Keywords Cladoceran subfossils · Carbon source · Nutrients · Climate change

Introduction

Global warming is degrading glaciers and permafrost at continental scales (Biskaborn et al. 2019). The second Chinese Glacier Inventory showed that, as a consequence of climate warming, the area of glaciers has decreased by ~17% in the 30 years since the first Chinese Glacier Inventory (Qiu 2010). Thawing of frozen material results in release of allochthonous organic carbon (OC) to downstream waters (Kendrick et al. 2018). It is estimated that ~48 Tg of dissolved inorganic carbon (DOC), of the 6 Pg of OC stored in the world's glaciers and ice-sheets, will be released in glacial runoff by 2050 (Hood et al. 2015). Aged (^{14}C -depleted) OC has been extensively recorded in Arctic (Guo et al. 2007), temperate (Zigah et al. 2017), and tropical rivers and lakes (Mayorga et al. 2005). A few field surveys provided evidence that aged allochthonous OC is nitrogen-rich, containing proteinaceous and other biologically derived compounds (Cameron et al. 2017), and can be consumed by microbial heterotrophs (Bellamy et al. 2017), invertebrates, and fish (Hågvar and Ohlson 2013; Fellman et al. 2015).

With recent anthropogenic activities and climate warming, not just OC, but also excess nutrients, are often delivered into rivers and lakes (Smol 2008). Watershed-derived nutrients can be transported to alpine lakes by glacial meltwater or precipitation.

Even more dramatically, rapid development of agriculture and industry in Asia has caused a nearly sixfold increase in the deposition rate of reactive N on parts of the Tibetan Plateau during the past 40 years (Zheng et al. 2002). In large parts of the world, the nitrogen deposition rate has reached $10 \text{ kg N ha}^{-1} \text{ yr}^{-1}$, exceeding the natural deposition rate by an order of magnitude (Zheng et al. 2002). The global atmospheric deposition rate of P can reach $50\text{--}100 \text{ g P ha}^{-1} \text{ yr}^{-1}$ (Mahowald et al. 2008). In addition, dust deposition may also supply alpine lakes with nutrients, particularly P (Mladenov et al. 2011), as a consequence of poor catchment vegetation development and relatively higher exposure to atmospheric deposition. These factors may lead to a rapid increase in nutrient concentrations in some high-altitude lakes. The rapid increase in nutrient abundance increases algal biomass and growth rates in lakes, which can result in eutrophication and alter food web structures.

Zooplankton play an important role in the carbon flow in aquatic ecosystems. The growth of zooplankton in aquatic ecosystems is supported mainly by autochthonous primary production (algae and aquatic plants) and terrestrial OC (Carpenter et al. 2005). In high-altitude regions, terrestrial OC consists mainly of aged (^{14}C -depleted) OC and contemporary terrestrial plant litter. The stock of aged OC mainly contains bacteria, ancient seeds preserved in glaciers and permafrost, and sometimes, combustion products (Stibal et al. 2008). There is a growing consensus that ancient allochthonous OC can be utilized by heterotrophic bacteria (Bellamy et al. 2017), and then partially fulfill consumer nutritional needs via the microbial loop (Nova et al. 2019).

Since most alpine lakes are fishless and strongly affected by environmental changes, zooplankton are sensitive to external forcing and become important indicator species for inferring long-term ecological changes in these lakes (Alric et al. 2013). Historical changes in zooplankton carbon sources are important not only for predicting the future structure of food webs in lakes, but also for explaining ecological processes, such as phytoplankton community change and top-down effects. Nevertheless, little information is available on long-term changes in the assimilation of autochthonous and allochthonous carbon by zooplankton and its climate- and environment-forcing mechanisms in high-altitude lakes. Fortunately, remains of many zooplankton species are well

preserved in lake sediment and can be used to track long-term changes in environmental forcing (Alric et al. 2013). In general, the occurrence of different zooplankton species has been shown to be closely related to limnological factors, such as lake depth and trophic state (Liu et al. 2008). For example, *Bosmina longirostris cornuta* and *Alona rectangula* are often abundant in relatively eutrophic waters (Liu et al. 2008). Analysis of zooplankton remains from high-altitude European and Himalayan lakes showed that the dynamics of *Daphnia* communities were mediated by the duration of ice-cover periods (Manca and Comoli 2004; Catalan et al. 2013). However, to date, zooplankton remains in lake sediments have only rarely been used to investigate long-term changes in zooplankton carbon sources.

To elucidate the historical changes in carbon sources for zooplankton and their response to climatic and environmental changes over the past thousand years, we analyzed the chitinous exoskeleton remains of subfossil cladoceran assemblages and their $\Delta^{14}\text{C}$ values in the sediment of alpine Lake Jirentso, on the Tibetan Plateau (TiP). Cladoceran exoskeletal remains, which are taxonomically diagnostic, consist mainly of chitin (Jeppesen et al. 2001; Kong et al. 2017). By studying the characteristics of cladoceran remains in the sediments, we were able to identify the species of cladocera that lived in the lake in the past, and their relative abundances, and to infer past environmental conditions. In addition, total nitrogen (TN) and total phosphorus (TP) in the sediments were used to infer past allochthonous nutrient inputs, and the diatom assemblage composition was used to infer past lake trophic state (Hu et al. 2014). Furthermore, titanium (Ti) in the sediment was used to infer soil and vegetation development in the catchment. Ti in sediments is a conservative element derived from soil input, and has been used to track catchment erosion and soil transport to lakes and their sediments (Chang et al. 2018).

We hypothesized that during cold periods, when alpine lakes were less productive, zooplankton consumed more cryosphere-derived OC. In contrast, with warming and increased nutrient concentrations, zooplankton utilized more contemporary, autochthonous OC. Our paleolimnological study provides a new approach for tracking shifts in the source of carbon for zooplankton and enables us to evaluate the forcing mechanisms during different historical periods.

Environmental setting

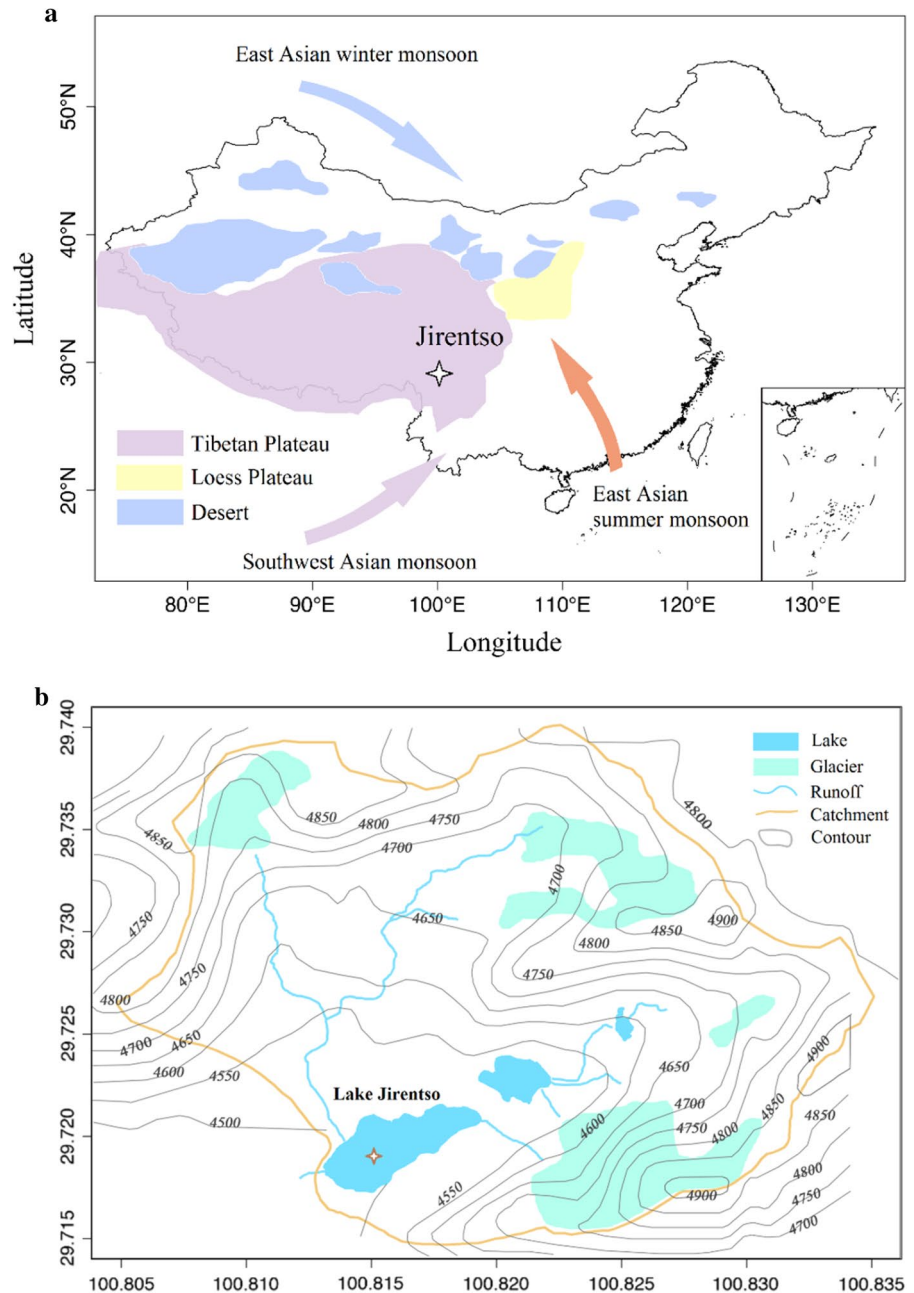
Lake Jirentso (29°41'N, 100°52'E, 4480 m above sea level) is located in Yajiang City, Sichuan, on the southeastern Tibetan Plateau (Fig. 1, Electronic Supplementary Material [ESM] Fig. S1). The lake has a surface area of 0.12 km² and a maximum depth of 28.5 m (Kong 2015). This remote oligotrophic lake (TN=0.12 mg L⁻¹, TP=0.007 mg L⁻¹) is minimally affected by direct human activities in the watershed, such as grazing and deforestation. However, the catchment is located near the Sichuan Basin, which is the most productive agricultural region in China. Fertilizer use has risen rapidly in Sichuan Province in recent decades (Sichuan Statistical Yearbook 2005). The catchment soil consists mainly of volcanic clastic rock rather than carbonate rock, thus avoiding “hard-water-lake dating error” caused by input to the lake of ¹⁴C-depleted bicarbonate from dissolution of local limestone (Cook et al. 2001). The lower slopes in the western and northwestern parts of the lake are populated with *Rhododendron pumilum* Hook. f. The catchment is affected by the Southwest Asian monsoon and the southern branch of the South Asian summer monsoon (Fig. 1). Rainfall amounts to approximately 730 mm during the summer monsoon season (May to September), according to monitoring data from the nearest meteorological station in Litang County, located ~38 km southwest of the lake. In the region, mean annual air temperature increased from 2.5 °C in 1953 to 4.6 °C in 2007, and during the same period, annual precipitation decreased by ~270 mm. Ground-based observations indicate that the glacier terminus in the Lake Jirentso catchment retreated at a rate of 10–30 m yr⁻¹ over the past 54 years (Li 2014). The duration of the ice cover in Lake Jirentso is about six months, from November to April.

Materials and methods

Sample collection and analytical methods

We collected a 46-cm-long sediment core in the deepest area (28 m) of Lake Jirentso in June 2017 using a HTH gravity corer. The core was sub-sectioned into 1-cm intervals on site. The naturally occurring radionuclide ²¹⁰Pb and the artificial radionuclide ¹³⁷Cs were measured in the sediment slices from

Fig. 1 Lake Jirentso is located on the Tibetan Plateau (TiP). **a** Impact of the Asian monsoon circulation on the climate of the TiP (Sun 1996). The star shows the location of Lake Jirentso. **b** The catchment of Lake Jirentso. The star represents the water sampling and sediment coring site



the upper part of the core (<24 cm), using standard gamma-ray spectroscopy (HPGe, GWL-120-15 detector). The age-depth model (ESM Fig. S2) for the past ~150 years was constructed using the constant rate of supply (CRS) model (Appleby 2001). Chronology for the older part of the core, below 24 cm depth, was constructed with accelerator mass spectrometry (AMS) ^{14}C dating of three terrestrial plant

macrofossils (ESM Table 1). Measured and calibrated ^{14}C ages are expressed in years before present (BP), i.e., before AD 1950. A Bayesian approach (R package Bacon) (Blaauw and Christen 2011) was used to perform age-depth modeling (Bacon manual v2.2). Based on the IntCal13 calibration curve (Reimer et al. 2013), the length between nodes (thick) was set to 2 and a total of 23 length units (sections) were

calculated when performing the modeling (ESM Fig. 3).

Radiocarbon and stable carbon isotope values of cladoceran remains in topmost sediment

Preparation and taxonomic identification of cladoceran remains followed standard protocols (Jiang and Du 1979; Szeroczyńska and Sarmaja-Korjonen 2007). For each sample, > 200 cladoceran individuals were enumerated. For the sample from the topmost sediment, 1 mg of remains (dry weight) was used to measure radiocarbon activity using the Accelerator Mass Spectrometry facility (Xi'an, China). The $\Delta^{14}\text{C}$ value was calculated by applying the following equation:

$$\Delta^{14}\text{C} (\text{‰}) = \delta^{14}\text{C} - 2(\delta^{13}\text{C} + 25) (1 + \delta^{14}\text{C}/1000)$$

$$\delta^{14}\text{C} = [(R_{\text{sample}}/R_{\text{standard}}) - 1] \times 1000\text{‰}$$

where $R = {}^{14}\text{C}/{}^{12}\text{C}$. The ${}^{14}\text{C}$ activity of oxalic acid II was used as R_{standard} . The analytical precision of $\Delta^{14}\text{C}$ was $\pm 3.7\text{‰}$. The stable carbon isotope values ($\delta^{13}\text{C}$) of the samples were determined using a Delta-Plus Advantage mass spectrometer (Finnigan MAT). The $\delta^{13}\text{C}$ was calculated according to the following equation:

$$\delta^{13}\text{C} = [(R_{\text{sample}}/R_{\text{standard}}) - 1] \times 1000\text{‰}$$

where $R = {}^{13}\text{C}/{}^{12}\text{C}$. The $\delta^{13}\text{C}$ of Vienna PeeDee Belemnite was used as an international standard. The analytical error ranged within $\pm 0.1\text{‰}$.

The $\delta^{13}\text{C}$ and $\Delta^{14}\text{C}$ of carbon sources

Dominant terrestrial plants (*Rhododendron pumilum* and *Kobresia*) were collected and cleaned with deionized water. An integrated water sample from 0 to 8 m in Lake Jirentso and surface water from the inflowing glacier streams were sampled with Niskin samplers. Particulate organic carbon (POC) samples were obtained by filtering water through a 0.7- μm Whatman GF/F filter (pre-combusted at 450 °C for 4 h) and then placed in aluminum foil and stored at -20 °C. Dissolved organic carbon (DOC) samples were collected from the filtered water and divided into two parts. One (50 mL) part was stored in amber

glass bottles at -20 °C and used for measuring $\delta^{13}\text{C}$ of DOC, and the other (2 L) part was freeze-dried to obtain a powdery sample for measuring the $\Delta^{14}\text{C}$ of DOC.

The $\Delta^{14}\text{C}$ of dissolved inorganic carbon (DIC) was used as a proxy for the $\Delta^{14}\text{C}$ of algae because the $\Delta^{14}\text{C}$ value of DIC biomass production tracks in situ DIC (Zigah et al. 2011, 2012). DIC samples were obtained from the filtered water (2 L) through a 0.7- μm Whatman GF/F filter and stored in gas-tight polypropylene Nalgene bottles, pre-cleaned with 10% HCl and deionized water, with zero headspace and sterilized with 100 μL saturated HgCl_2 solution (Fellman et al. 2015). The $\delta^{13}\text{C}$ of algae was determined using the $\delta^{13}\text{C}$ of phospholipid fatty acids (PLFAs) of algae. PLFAs were extracted from lake POC samples using a modified Bligh and Dyer method (Dickson et al. 2009) and then derivatized using mild alkaline transmethylation to generate fatty acid methyl esters (FAME) (Boschker et al. 2005). GC-MS (Thermo Finnigan Trace) was used to identify compounds. GC combustion isotope ratio mass spectrometry (GC-c-IRMS, using a Trace GC Ultra GC apparatus, Thermo Finnigan) was applied to determine the $\delta^{13}\text{C}$ of individual FAMEs. The $\delta^{13}\text{C}$ of 18:3 ω 3 and 20:5 ω 3 PLFAs was corrected and then used as a proxy for the $\delta^{13}\text{C}$ of algae (Middelburg 2014).

Isotope mixing model

We used a four-component IsoSource model (Phillips and Gregg 2003), combining $\delta^{13}\text{C}$ and $\Delta^{14}\text{C}$ to estimate the relative contribution of different carbon sources used by cladocerans in the most recent year (ca. 2010). The model is based on mass conservation of stable isotopes and superimposes all possible percentage combinations of the resources according to the specified increment range. The frequency of occurrence of each resource contribution percentage is analyzed to obtain the optimal solution. In this study, the values of the source increment and the mass balance tolerance were set to 1% and 0.05‰, respectively. The four potential carbon sources, which include algae, terrestrial plants, POC, and DOC from inflowing glacier streams, were chosen as endmembers. Individual terrestrial plant taxa were lumped into the category “terrestrial plants.” Aquatic plants were excluded because of their extremely low biomass in Lake Jirentso. In addition, POC and DOC in

the inflowing glacier streams are derived mainly from glaciers and frozen soils, and have highly depleted $\Delta^{14}\text{C}$ values. Terrestrial plants fix ^{14}C -enriched atmospheric CO_2 through photosynthesis and therefore have much higher $\Delta^{14}\text{C}$ values than aged OC in glacier streams.

Other paleoclimate and paleoenvironment proxies

The organic C:TN ratio (C:N) of the sediment core was quantified using an Elemental Analyzer. The total phosphorus concentration in the sediment was measured using an inductively coupled plasma atomic emission spectrometer (ICP-AES). Ti concentration was analyzed with inductively coupled plasma-mass spectrometry (ICP-MS). The long-term mean annual air temperature in the studied region was reconstructed using the ECHO-G model (Kuang et al. 2008), based on instrumental data recorded since 1960 at the nearby Xiaojin County meteorological station in Sichuan Province ($30^\circ35'–31^\circ43'\text{N}$, $102^\circ01'–102^\circ59'\text{E}$), located ~240 km from Lake Jirentso. The coupled ECHO-G model was developed based on the spectral atmospheric model ECHAM4 and the global ocean circulation model HOPE-G (Legutke and Voss 1999). ECHAM4 is the fourth-generation atmospheric general circulation model based on original equations with a mixed p - σ coordinate system. The horizontal resolution of the model is about $3.75^\circ \times 3.75^\circ$. The vertical resolution consists of 19 levels and includes five upper levels above 200 hPa, covering high-altitude regions. The horizontal resolution of the ocean model HOPE-G is approximately $2.8^\circ \times 2.8^\circ$. The vertical resolution is 20 levels (Wolff et al. 1997). The ECHAM4 and HOPE-G are coupled using the coupler OASIS3.

The $\delta^{18}\text{O}$ values in rain and stalagmite carbonate can serve as proxies for regional-local rainfall amount (Orland et al. 2015). It has been reported that Chinese stalagmite $\delta^{18}\text{O}$ records reflect changes in the Asian monsoon intensity and a first-order change in spatially integrated rainfall between moisture sources and cave position on orbital to millennial time scales (Cheng et al. 2016). In our study, a precipitation index was reconstructed using speleothem $\delta^{18}\text{O}$ records from Shenqi Cave (Tan et al. 2018), also located in Sichuan Province. Tan et al. (2018) drilled out stalagmite samples at intervals of 0.5–1 mm, in which they measured $\delta^{18}\text{O}$. The stalagmite $\delta^{18}\text{O}$ was

negatively correlated with rainfall amount in this area during 1951–2010 AD (Leshan Station, 95 km northeast of Shenqi Cave). They then used the negative principal component analysis value as a synthesized precipitation index for southwest China, with a resolution of five years. A high precipitation index means a large rainfall amount. Despite differences across different stalagmite records at the multi-decadal scale, the long-term monsoon rainfall trend was similar throughout southwest China (Xiao et al. 2014; Tan et al. 2018).

To reconstruct past trophic state in Lake Jirentso, we analyzed the composition of the diatom assemblage. The preparation and identification of diatom microfossils followed standard methods (Battarbee et al. 2001), and at least 300 diatom valves were counted for each sample. The accumulation rate of cladocerans and diatoms was calculated by multiplying the number of cladocerans or diatoms per unit dry mass (number g^{-1} dry), times the bulk dry mass accumulation rate ($\text{g dry cm}^{-2} \text{yr}^{-1}$).

Statistical analysis

Climate and environment are often considered to be the primary drivers of ecological change in alpine lakes, because of the close link between biological groups and temperature fluctuations and nutrients (Catalan et al. 2013). Therefore, we chose environment variables TOC, TN, TP, C:N mass ratio (wt/wt), Ti, annual mean air temperature, and the precipitation index as predictor variables in this study. The main trends in the cladoceran assemblage composition and the environmental proxies were extracted using an exploratory detrended correspondence analysis (DCA). The gradient length was short ($< 2 \text{ SD}$), indicating that Redundancy Analysis (RDA) would be statistically appropriate for exploring the relationship between the cladoceran records and the environmental variables (Wang et al. 2020). RDA analyses were performed using CANOCO 4.5 software. Unrestricted Monte Carlo permutation was used to test the significance of each variable. A set of significant explanatory variables was automatically selected, and then collinear parameters ($\text{VIF} \geq 20$) were eliminated to further select the most significant environmental proxies ($p < 0.05$). The relationship between the cladoceran accumulation rate and environmental variables was investigated using the Statistical Program for

Social Sciences (SPSS) 20.0 software. Significance differences in values of variables between different periods were examined with one-way ANOVA, followed by an LSD test that used a *p*-value of 0.05.

Results

Paleoecological records

Paleoecological records of the past ~950 years have documented a warm period in China, the Medieval Warm Period (MWP, AD 931–1320) (Fig. 2a), most pronounced in the centuries during the Song-Yuan Dynasties (AD 960–1368) (Ge et al. 2013). In south China, the MWP was accompanied by relatively high air temperature and high precipitation index (mean value – 0.19) (Fig. 2b) (Tan et al. 2018). The relatively high Ti contents (mean value 3.2 g kg⁻¹) in the lake sediments deposited during the MWP corresponded to strong wash-off of Ti from the catchment (Fig. 3c). The concentration of P in the sediment

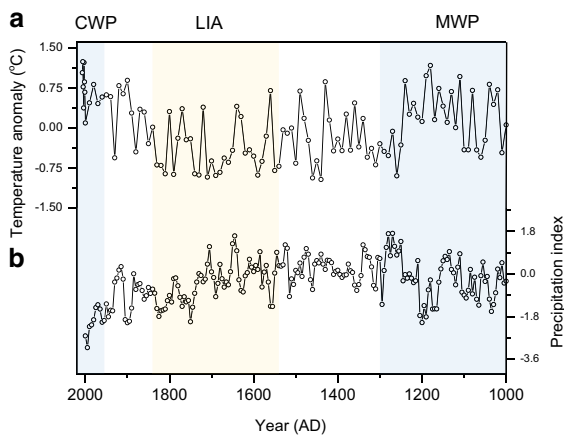


Fig. 2 Reconstructed air temperatures and Asian summer monsoon rainfall during the past ~1000 years on the southeastern TiP. **a** Reconstruction of annual air temperature using the ECHO-G model, based on instrumental data from the meteorological station in Xiaojin County, located ~240 km from Lake Jirentso. The temperature anomaly refers to the difference between the annual average temperature and the average temperature of the past ~1000 years. **b** The reconstructed precipitation index of Asian summer monsoon rainfall, based on speleothem δ¹⁸O records from the Shenqi Cave on the southeast margin of the TiP (Tan et al. 2018). Blue-gray shading indicates the Medieval Warm Period (MWP) and the Current Warm Period (CWP) over the past ~1000 years in China. Faint yellow shading indicates the Little Ice Age (LIA)

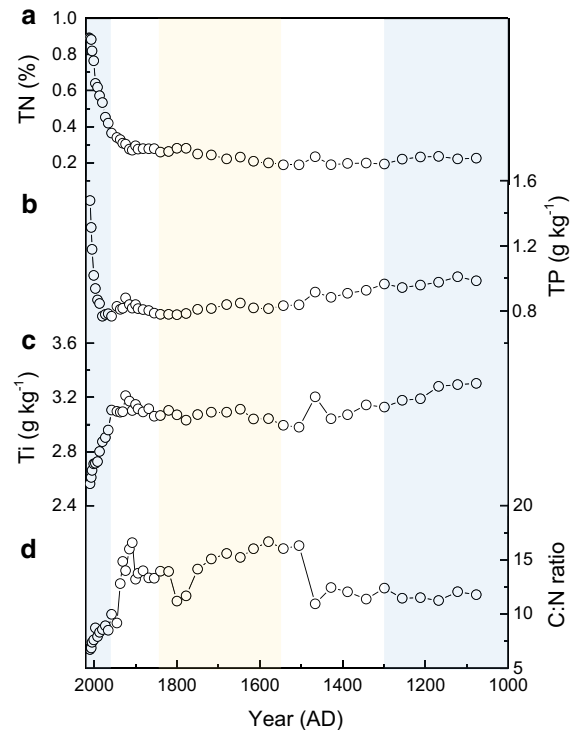


Fig. 3 Geochemical proxies in the lake sediment core from Lake Jirentso and the speleothem δ¹⁸O records from Shenqi Cave on the southeast margin of the Tibetan Plateau. **a–b** Trends in total phosphorus (TP) and total nitrogen (TN) content in the Lake Jirentso sediment core, showing a sharp increase since the 1960s. **c–d** Trends in the content of Ti and the C:N ratio in the Lake Jirentso sediment core

during the MWP ($0.97 \pm 0.02 \text{ g kg}^{-1}$) was slightly higher than during the cooler Little Ice Age (LIA, AD 1550–1850) ($0.81 \pm 0.02 \text{ g kg}^{-1}$) ($p < 0.001$, Fig. 3). The mean value of C:N ratios in the sediment core was 11.7 ± 0.4 during the MWP, after which the value generally increased to 14.5 ± 1.5 during the LIA (Fig. 3). The mean precipitation index during the LIA was -0.41 .

The current anthropogenic warming period (CWP), which began around the 1960s in this region (Figs. 2a and 4e), stands in stark contrast to the conditions that prevailed in the LIA on the TiP. The CWP was accompanied by lower mean precipitation index (-1.69) (Fig. 2b) and mean Ti content (2.7 g kg^{-1}) (Fig. 3c) compared to the MWP and the LIA. The C:N ratios in the sediment core showed a rapid downward trend during the CWP, varying in the range 6.7–8.9. The striking increase in TN and TP

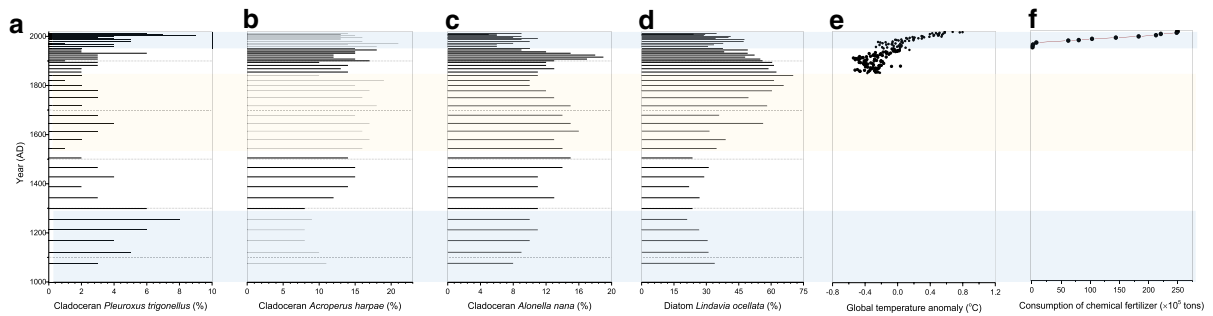


Fig. 4 Long-term trends in cladoceran and diatom assemblage composition in the Lake Jirentso sediment core, compared with global mean air temperature and use of chemical fertilizers in Sichuan Province over recent decades. **a–c** Relative abundances of some key cladoceran taxa including the temperate/subpolar species *Pleuroxus trigonellus* **a**, the Arctic/polar species *Acroperus harpae* **b**, both well-documented indicators of cold periods with longer periods of ice cover, and enhanced abundance of the oligotrophic cladoceran *Alonella nana* **c**, indicating low nutrient contents. **d** Relative abundances of the planktonic diatom taxon *Lindavia ocellata*, indicating low

nutrient concentrations (Chen 2015). **e** Trends in global mean temperature (Stocker et al. 2013), synchronized with the temperature change over the past 60 years, monitored at the nearby meteorological station in Litang County, located ~38 km southwest of the lake. **f** Rapid increase in the consumption of chemical fertilizers in Sichuan, based on statistical yearbook data from Sichuan Province. Upper blue-gray shading indicates the Current Warm Period and the lower blue-gray shading the Medieval Warm Period. Faint yellow shading indicates the Little Ice Age (LIA)

and decline in C:N ratios is unprecedented during the CWP in the records. Concentrations of TN and TP reached 0.89% and 1.5 g kg⁻¹, respectively, ca. 2010.

Cladoceran remains and diatom assemblages

A total of 12 cladoceran species were identified in the sediments (Fig. 4 and ESM Fig. S4). The dominant taxa were littoral cladocerans, such as *Alona guttata*, *Alona rectangular*, *Alona affinis*, *Alonella nana*, *Acroperus harpae*, *Chydorus sphaericus*, and *Pleuroxus trigonellus*. Only a few planktonic species, including *Daphnia longispina* and *Bosmina* sp., were recorded in the warm periods. In addition, diatom records showed that the dominant diatom taxa were planktonic *Lindavia ocellata* and small fragilarioid species, such as *Staurosira construens* and *Staurosirella pinnata* (ESM Fig. S5). Other benthic and epiphytic species included *Achnanthyidium minutissimum* and *Nitzschia fonticola*.

The structure and abundance of the cladoceran assemblages changed over time (ESM Fig. S4). The mean relative abundance of the cladoceran *Pleuroxus trigonellus*, typical in temperate/subpolar waters (Kong et al. 2017), was $5.3 \pm 1.8\%$ ($n=6$) during the MWP, which was significantly higher than in the LIA ($2.3 \pm 0.8\%$, $n=12$, $p < 0.001$) (Fig. 4a). In contrast, the mean abundance of the cold-water species

Acroperus harpae (Lotter et al. 1998) during the MWP ($9.0 \pm 1.3\%$, $n=6$) was significantly lower than in the LIA ($15.8 \pm 2.3\%$, $n=12$, $p < 0.001$) (Fig. 4b). Marked shifts in dominance between temperate and cold-water taxa conformed to mean annual air temperature reconstructions using the ECHO-G model based on the data collected from the nearby meteorological station in Xiaojin County since 1960 (Fig. 2a). In addition, the mean relative abundance of the cladoceran *Alonella nana*, typical in oligotrophic waters (Bjerring et al. 2009) during the MWP ($9.8 \pm 1.1\%$, $n=6$), was lower than during the LIA ($13.2 \pm 2.0\%$, $n=12$) ($p < 0.05$) (Fig. 4c). During the LIA, the average relative abundance of benthic diatoms was 33.3%, and that of planktonic diatoms was 66.7% (ESM Fig. S5). In contrast, the average relative abundance of benthic diatoms (60.1%) was significantly higher than planktonic diatoms (37.7%) ($p < 0.001$) during the MWP. In addition, the abundance of the oligotrophic planktonic diatom *Lindavia ocellata*, a taxon that is typically more abundant at low nutrient levels (Saros and Anderson 2015), was relatively low during the MWP (Fig. 4d).

During the CWP, the accumulation rate of all diatoms and the relative abundance of benthic fragilarioid species increased simultaneously (ESM Fig. S5), along with synchronous dramatic increases in N and P concentrations during this period (Fig. 3).

Furthermore, the rapid decline of oligotrophic cladocerans such as *Alonella nana* occurred simultaneously with the abrupt increase in N and P concentrations (Fig. 3). At the same time, an increased relative abundance of the temperate cladoceran *Pleuroxus trigonellus* was observed (ESM Fig. S4). The increased accumulation rate of all cladocerans and the enhanced relative abundance of planktonic species, e.g., *Bosmina longirostris* and *Daphnia longispina*, suggest increased food resources and a longer growing season (reduced ice cover).

Environmental driving factors of cladoceran communities

In the RDA analyses of interactions between the relative abundance of cladocerans and the environmental variables, we found that C:N ratio, TP concentration, and annual mean air temperature were most strongly correlated with the assemblage data ($p < 0.05$) (Fig. 5). The first axis (0.28) and the second axis (0.06) explained 34% of the environmental information with respect to the relative abundance of cladocerans. Samples from the MWP and the CWP were distributed along the positive direction of axis 1, corresponding to the variables TP and annual mean air temperature. Moreover, the most important environmental factor affecting cladoceran community composition from the 1960s to the early 1990s was

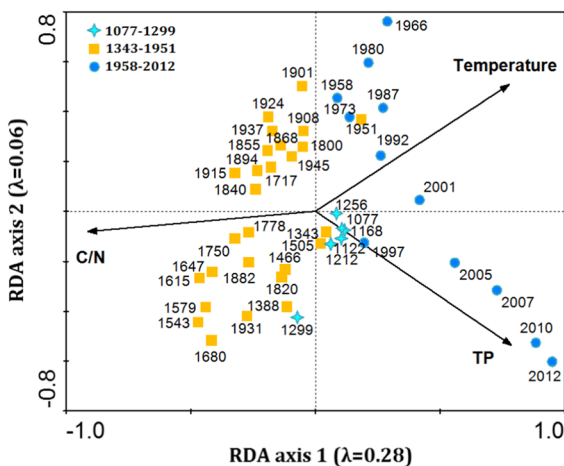


Fig. 5 The ordination bi-plot with the Redundancy Analysis (RDA) of cladoceran assemblage composition during the period ~1077–2012 AD. Temperature is the annual mean air temperature

the annual mean air temperature, whereas the most important factor from the 1990s onward shifted to TP. In contrast, samples from the LIA were in the opposite direction of the mean annual temperature variable. In addition, accumulation rates of all cladocerans correlated positively with air temperature ($r = 0.71$, $p < 0.001$) and negatively with the C:N ratio in the sediment core ($r = -0.61$, $p < 0.001$) (Fig. 6). Overall, increased air temperature and nutrient inputs triggered pronounced changes in cladoceran assemblage composition and abundance.

Recent contribution of carbon sources to cladocerans

The $\delta^{13}\text{C}$ and $\Delta^{14}\text{C}$ values of cladoceran remains in the topmost sediment (ca. 2010) were -27.7‰ and -71.7‰ , respectively (Fig. 7). The $\delta^{13}\text{C}$ and $\Delta^{14}\text{C}$ values of four potential carbon sources for zooplankton, including modern terrestrial plants, POC and DOC from inflowing rivers ($\text{POC}_{\text{inflow}}$ and $\text{DOC}_{\text{inflow}}$), and phytoplankton in the lake,

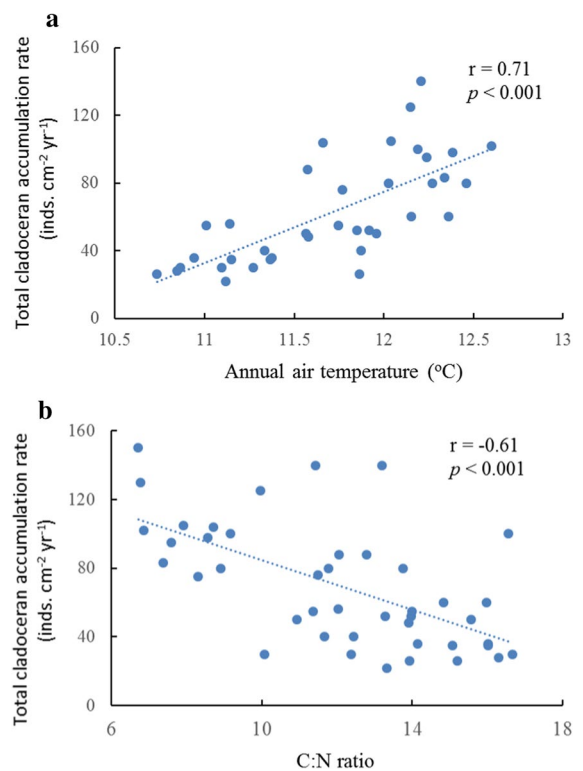


Fig. 6 Linear regression between annual mean air temperature **a** and C:N ratio in the sediment core **b** versus total cladoceran accumulation rate

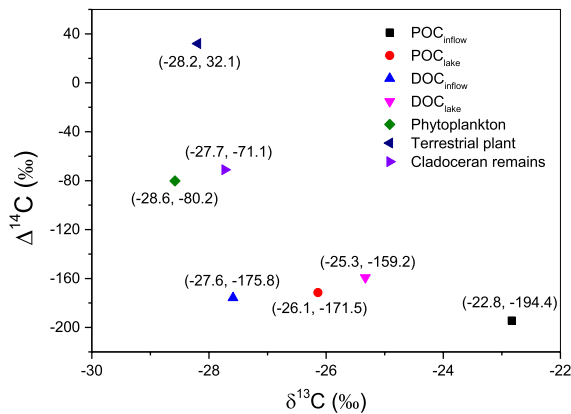


Fig. 7 Plots of $\delta^{13}\text{C}$ and $\Delta^{14}\text{C}$ values from cladoceran remains in the top of the sediment core, and ancient and newly produced carbon in Lake Jirentso and its inflow stream. $\text{POC}_{\text{inflow}}$ and $\text{DOC}_{\text{inflow}}$ represent particulate and dissolved organic carbon in the inflow stream. POC_{lake} and DOC_{lake} indicate particulate and dissolved organic carbon in the lake water, respectively. The $\Delta^{14}\text{C}$ value of dissolved inorganic carbon is used as a substitute for $\Delta^{14}\text{C}$ of algae. The $\delta^{13}\text{C}$ of phospholipid fatty acid biomarkers of algae was measured to determine the $\delta^{13}\text{C}$ of algae

were measured. Among those sources, the $\delta^{13}\text{C}$ and $\Delta^{14}\text{C}$ values of modern terrestrial plants were -28.2‰ and $+32.1\text{‰}$. $\text{POC}_{\text{inflow}}$ and $\text{DOC}_{\text{inflow}}$ had $\delta^{13}\text{C}$ values of -22.8‰ and -27.6‰ , and $\Delta^{14}\text{C}$ values of -194.4‰ and -175.8‰ , respectively. Phytoplankton $\delta^{13}\text{C}$ value was -28.6‰ . The $\Delta^{14}\text{C}$ value of DIC in lake water (a proxy for phytoplankton) was -80.2‰ . The $\Delta^{14}\text{C}$ values of the most recent cladoceran remains and potential carbon sources for cladocerans, except for terrestrial plants, correspond to conventional radiocarbon ages ranging from 671 to 1735 years BP.

Based on the $\delta^{13}\text{C}$ and $\Delta^{14}\text{C}$ values of recent cladoceran remains in the sediment and those of potential carbon sources for cladocerans in the water, we estimated the relative contributions of four carbon sources. The IsoSource mixing model exercise revealed that the mean contributions of riverine POC and DOC, algae, and terrestrial-plant-derived OC to the carbon sources for cladocerans were 9%, 20%, 36.7%, and 34.3%, respectively, around 2010 (ESM Table S2).

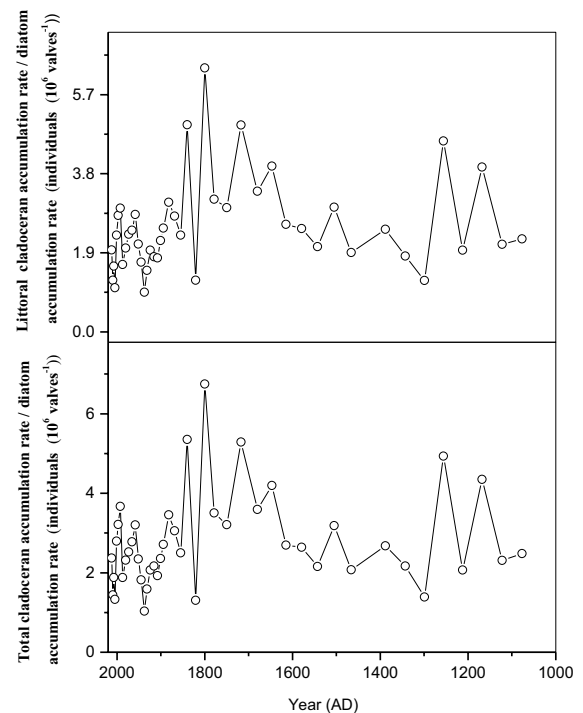


Fig. 8 The ratio of the total and littoral cladocerans accumulation rates to the total diatom accumulation rate in the sediment core from Lake Jirentso

Ratio of cladoceran:diatom accumulation rate

The zooplankton:phytoplankton biomass ratio can be employed to indicate the feeding pressure of zooplankton on phytoplankton (Søndergaard et al. 2008). This ratio is highly sensitive to fish predation on zooplankton and decreases markedly with increasing predation (Jeppesen et al. 2011), but our study lake is fishless. Considering that the accumulation rate change can be used to reflect the biomass change in paleolimnological studies (Kong 2015), we used the cladoceran:diatom accumulation rate ratio to track the amount of phytoplankton that can be consumed by cladocerans during historical periods. The mean values of the ratios of the total and littoral cladoceran accumulation rates relative to the diatom accumulation rate during the LIA were 3.8 ± 1.6 and 3.6 ± 1.5 individuals $(10^6 \text{ valves}^{-1})$ ($n=12$), respectively, which were significantly higher than the corresponding ratios of 2.4 ± 0.7 and 2.0 ± 0.6 individuals $(10^6 \text{ valves}^{-1})$ ($n=11$) during the CWP ($p < 0.05$) and 3.2 ± 1.3 and 3.0 ± 1.2

individuals (10^6 valves)⁻¹ ($n=6$) during the MWP ($p < 0.05$) (Fig. 8).

Discussion

Our findings provide compelling evidence that both autochthonous and allochthonous OC contributed to the food resources of zooplankton in our study lake, but their contribution to the diet differed among the different historical periods. Climate change and nutrient concentrations were important driving forces for changes in cladoceran assemblage composition and food resources.

Food sources for zooplankton

During the LIA, low temperatures and low nutrient concentrations reduced the biomass of algae and zooplankton. Low temperatures also indicate less melt of old glacial ice. Nonetheless, a relatively wet climate and abundant summer monsoon rainfall in the LIA (Tan et al. 2018) may still have led to abundant soil OC being delivered to the lakes. This was supported by the relatively high C:N ratios (14.5 ± 1.5) in the sediments deposited during the LIA (Fig. 6). This ratio is often used to indicate the origin of the organic carbon. Ratios in the core during the LIA were within the range of soil (5–10.7) and terrestrial plants (14–23) (Meyers and Teranes 2001; Holtvoeth et al. 2016), indicating a dominant terrestrial source for the OC in the Lake Jirentso sediments. Higher cladoceran:diatom accumulation rate ratios during the LIA also suggested that less autochthonous food was available per cladoceran than during the warm periods (Fig. 8) and low abundances or absence of *Daphnia* (ESM Fig. S4) pointed in the same direction. Since the low air temperatures during the LIA were not conducive to terrestrial vegetation growth, zooplankton likely consumed more aged terrestrial OC.

The higher temperature and slightly higher concentration of sedimentary P during the MWP than the LIA likely stimulated algal growth (Fig. 3 and ESM Fig. S5). However, the relatively high total cladoceran:diatom accumulation rate ratios during the MWP indicated that algal biomass was most likely still insufficient to fulfill zooplankton dietary needs (Fig. 8). In addition, the C:N ratios of the sediment core during the MWP were close to those of soil organic matter (Fig. 3). Therefore,

zooplankton likely relied, in part, on aged soil OC as a food resource.

In contrast, the lowest cladoceran:diatom accumulation rate ratios during the CWP indicated that more autochthonous food resources were available for the zooplankton than during the LIA and the MWP. Low C:N ratios (6.7–8.9) during the CWP indicated a mixed algal (6–7) and soil (5–10.7) source for the OC (Meyers and Teranes 2001; Holtvoeth et al. 2016). The dramatic increase of N input not only led to the decline in C:N ratio, but also promoted the growth of algae in the lake. The remarkable increases in total sediment cladoceran and diatom accumulation rates in recent decades reflect greater algae resources and a longer growing season. Consequently, the contribution of algae to the food of cladocerans during the CWP was probably higher than before. In addition to algae, ancient OC from glacier runoff and permafrost meltwater might have been an additional food resource for zooplankton. This is supported by the estimated high contribution of algae (36.7%) and riverine OC (29%) to cladocerans in the sediment ca. 2010 (ESM Table S2). The unprecedented low Ti values in recent decades indicate that the basin vegetation was well developed, and subsidized the lake carbon pool, which was an important contributor (34.3%) to the carbon source of zooplankton.

Generally, the primary factors that affect the contribution of carbon sources to zooplankton are food quantity, quality, and diversity (Taipale et al. 2014). Zooplankton typically prefer algae as a food source, as they possess a higher nutritional value than terrestrial OC (Taipale et al. 2014). Nevertheless, the somatic growth and reproduction of zooplankton require a range of substances. Terrestrial materials lack polyunsaturated fatty acids and sterols, but contain abundant saturated fatty acids and mineral elements, which are important for the biological processes of zooplankton, such as catabolism and crustacean carapace or exoskeleton growth (Jeziorski et al. 2012). The food composition of zooplankton likely changed with changes in the prevailing environmental conditions. However, algae will, in most cases, still be the preferred food item for zooplankton.

Climate change and nutrient concentrations mediate zooplankton assemblages and food resources

Shifts in carbon assimilation by cladocerans reveal that climate and environmental driving forces have

high impacts on ecosystem structure and function. In the long term, climate is often regarded as a major driving force of ecological change in polar and alpine lake ecosystems, since temperature fluctuations change the duration of ice cover, the heat budget and nutrient recycling in those lakes (Catalan et al. 2013). In addition, even a slight increase in nutrient concentrations in remote high-altitude lakes can lead to an increase in primary production (Hu et al. 2014), thereby influencing zooplankton biomass and assemblages through several processes, including the bottom-up effects of the microbial loop. Our RDA results further confirmed that mean annual air temperature, TP, and factors linked to changing C:N ratios significantly influenced the cladoceran assemblages in Lake Jirentso (Fig. 5). The accumulation rate of all cladocerans correlated positively with air temperature and negatively with the C:N ratio in the sediment core (Fig. 6), indicating that increased air temperature and nutrient inputs triggered pronounced changes in cladoceran assemblage composition and accumulation.

Lake Jirentso is not only replenished by snow melt water and precipitation, but also by meltwater from small glaciers in the basin. The relatively short growing season and the maintenance of low water temperature in summer and autumn may reduce the growth of planktonic species. High water clarity also favours benthic algae growth, even in relatively deep lakes (Vadeboncoeur et al. 2003). Therefore, the cladoceran assemblage in this lake was dominated by littoral species over the past ~950 years. Low cladoceran accumulation rates during the LIA were associated with a cold-water environment, extended periods of ice cover, and a very short growing season. Furthermore, the area of glaciers and snow cover expanded, and dust source areas decreased, thereby causing a decrease in dust-derived P concentration (Yao et al. 2004). Low nutrient concentrations during the LIA were supported by high abundances of the oligotrophic diatom *Lindavia ocellata* and the cladoceran *Alonella nana*, and low abundance of *Daphnia longispina* (Fig. 4). Importantly, the vast majority of cladoceran taxa in this period were littoral species, which likely reflected habitat changes linked to longer periods of ice cover. Low temperatures, combined with low nutrient concentrations, resulted in low algal and cladoceran biomass. The feeding pressure of littoral cladocerans on benthic algae likely caused the dominance of planktonic diatoms at that time.

During the MWP, the concentration of P in the sediment was significantly lower than during the CWP ($p < 0.001$, Fig. 3), indicating less P was supplied from eroded catchment soil during the MWP than during the CWP. Furthermore, stronger summer monsoon rainfall intensity during the MWP reduced the dry deposition of P (Fig. 2). Less P input resulted in lower algal biomass during the MWP, so less algae were available for cladocerans.

In contrast to the MWP, anthropogenic warming since the 1960s initiated different responses in terms of zooplankton assemblage composition and their carbon sources. The cladoceran community composition from the 1960s to the early 1990s was mainly impacted by the annual mean temperature, whereas the key factor from the 1990s onward shifted to TP (Fig. 5). Abundant accumulation of N and P in the top of the Lake Jirentso sediment core (Fig. 3) indicates increased nutrient delivery to the lake in recent years, likely linked to the increased fertilizer use in Sichuan Province over the last three decades (Fig. 4f), regional industrial emissions, and deposition of dust. The elevated nitrate concentration in the ice core from the TiP follows a trend similar to that of TN in the sediment core from Lake Jirentso (Thompson et al. 2000), reflecting enhanced regional atmospheric nutrient deposition. The mean N deposition rate in the Sichuan Basin was as high as $40 \text{ kg ha}^{-1} \text{ yr}^{-1}$ during 2005–2009 (Zhang et al. 2012). It is estimated that 1.8 million tons of P are related to combustion emissions in the global atmospheric P budget (Wang et al. 2015). Weaker summer monsoon rainfall intensity and wind strength during the CWP favored the dry deposition of nutrients. Moreover, higher temperature would have enhanced the duration and stability of water-column thermal stratification, thereby enhancing nutrient cycling in the epilimnion and favoring dominance by eutrophic diatom and cladoceran taxa.

Although P in sediments is potentially mobile, the accumulation rates of cladocerans and diatoms showed highly synchronous trends with P concentrations in the sediment from Lake Jirentso, and the accumulation rates of all diatoms correlated positively with the P concentration ($r = 0.55$, $p < 0.001$) (ESM Fig. S6). In addition, with warming during the CWP, more zooplankton could have moved and fed in the open water, concurrent with increasing phytoplankton

growth. Consequently, there was a shift from littoral cladoceran taxa to more planktonic species, including *B. longirostris* and *D. longispina* during the CWP.

Historical changes in zooplankton carbon sources over the past millennium are relevant for predictions of future changes in lake food webs. Overall, anthropogenic climate warming and enhanced nutrient concentrations will have profound implications for the carbon source composition of zooplankton. In this context, the food web structure of lakes, which is closely linked to the cryosphere, may be largely sustained by freshly produced OC. If the ratio between zooplankton and algae in lakes becomes lower in the future, algae growth will be less controlled by zooplankton and the risk of algae blooms may increase (Søndergaard et al. 2008). Understanding the changes in zooplankton carbon sources and the driving forces that influence these changes will undoubtedly be helpful for developing lake management strategies, especially with respect to the stability and biodiversity of high-altitude and polar lake ecosystems.

Conclusions

We found that the carbon source composition of zooplankton in Lake Jirentso varied over time and was mainly influenced by climate change and nutrient concentrations. Relatively high diatom accumulation rates and low cladoceran:diatom accumulation rate ratios during the CWP indicated that more contemporary autochthonous food resources were available for the zooplankton with warming. In contrast, during the LIA, the high cladoceran:diatom accumulation rate ratios reflected that cladocerans assimilated more allochthonous OC to replenish their food because of low autochthonous primary production under low temperature and low nutrient concentrations. Paleolimnological studies enable analyses of the shifting balance between aged, cryosphere-derived OC and contemporary OC, to zooplankton, and forcing mechanisms for OC sources during warming and cold periods. They also provide a way to discern the role of anthropogenic nutrient emissions in the changing modern environment.

Acknowledgements We acknowledge XD Yang, Y Chen, and L Liu for field assistance, LY Kong and S Min for assistance in ECHO-G modeling, and LC Tan for sharing data on

oxygen isotopes. The “Pioneer” and “Leading Goose” R&D Program of Zhejiang (2022C02038), National Science Foundation of China (31971475, 31930074, and 31770509), and the China-Netherlands Joint Programme (JSTP) (GJHZ05) supported this publication. JJM was supported by the Netherlands Earth System Science Center. EJ was supported by the Tübitak outstanding researchers program, BIDEB 2232 (project 118C250).

References

- Alric B, Jenny JP, Berthon V, Arnaud F, Pignol C, Reyss JL, Sabatier P, Perga ME (2013) Local forcings affect lake zooplankton vulnerability and response to climate warming. *Ecology* 94:2767–2780
- Appleby PG (2001) Chronostratigraphic techniques in recent sediments. In: Last WM, Smol JP (eds) Tracking environmental change using lake sediments: basin analysis, coring, and chronological techniques, vol 1. Kluwer Academic Publishers, Dordrecht, pp 171–203
- Battarbee RW, Jones VJ, Flower RJ, Cameron NG, Bennion H, Carvalho L, Juggins S (2001) Diatoms. In: Last WM, Smol JP (eds) Tracking environmental change using lake sediments Terrestrial algal and siliceous indicators, vol 3. Kluwer Academic Publishers, Dordrecht, pp 155–202
- Bellamy AR, Bauer JE, Grotto AG (2017) Influence of land use and lithology on sources and ages of nutritional subsidies to stream macroinvertebrates: a multi-isotopic approach. *Aquat Sci* 79:925–939
- Biskaborn BK, Smith SL, Noetzli J, Matthes H, Vieira G, Streletskiy DA et al (2019) Permafrost is warming at a global scale. *Nat Commun* 10:264
- Bjerring R, Becares E, Declerck S, Gross EM, Hansson LA, Kairesalo T, Nykänen M, Halkiewicz A, Kornijów R, Conde-Porcuna JM, Seferlis M, Nöges T, Moss B, Amsinck SL, Odgaard BV, Jeppesen E (2009) Subfossil Cladocera in relation to contemporary environmental variables in 54 Pan-European lakes. *Freshw Biol* 54:2401–2417
- Blaauw M, Christen JA (2011) Flexible paleoclimate age-depth models using an autoregressive gamma process. *Baye Anal* 6:457–474
- Boschker HTS, Kromkamp JC, Middelburg JJ (2005) Biomarker and carbon isotopic constraints on bacterial and algal community structure and functioning in a turbid, tidal estuary. *Limnol Oceanogr* 50:70–80
- Cameron KA, Stibal M, Hawkins JR, Mikkelsen AB, Telling J, Kohler TJ, Gözdereliler E, Zarsky JD, Wadham JL, Jacobsen CS (2017) Meltwater export of prokaryotic cells from the Greenland ice sheet. *Environ Microbiol* 19:524–534
- Carpenter SR, Cole JJ, Pace ML, Van de Bogert M, Bade DL, Bastviken D, Gille CM, Hodgson JR, Kitchell JF, Kritzberg ES (2005) Ecosystem subsidies: terrestrial support of aquatic food webs from ¹³C addition to contrasting lakes. *Ecology* 86:2737–2750
- Catalan J, Pla-Rabés S, Wolfé AP, Smol JP, Rühland KM, Anderson NJ, Kopáček J, Stuchlík E, Schmidt R, Koinig KA, Camarero L, Flower RJ, Heiri O, Kamenik C,

- Korhola A, Leavitt PR, Psenner R, Renberg I (2013) Global change revealed by palaeolimnological records from remote lakes: a review. *J Paleolimnol* 49:513–535
- Chang J, Zhang E, Liu E, Sun W, Langdon PG, Shulmeister J (2018) A 2500-year climate and environmental record inferred from subfossil chironomids from Lugu Lake, southwestern China. *Hydrobiologia* 811:1–14
- Cheng H, Edwards RL, Sinha A, Spötl C, Yi L, Chen S, Kelly M, Kathayat G, Wang XF, Li XL, Kong XG, Wang YJ, Ning YF, Zhang HW (2016) The Asian monsoon over the past 640,000 years and ice age terminations. *Nature* 534:640–646
- Cook GT, Bonsall C, Hedges REM, McSweeney K, Boronean V, Pettitt PB (2001) A freshwater diet-derived C-14 reservoir effect at the stone age sites in the iron gates gorge. *Radiocarbon* 43:453–460
- Dickson L, Bull ID, Gates PJ, Evershed RP (2009) A simple modification of a silicic acid lipid fractionation protocol to eliminate free fatty acids from glycolipid and phospholipid fractions. *J Microbiol Methods* 78:249–254
- Fellman JB, Hood E, Raymond PA, Hudson J, Bozeman M, Arimitsu M (2015) Evidence for the assimilation of ancient glacier organic carbon in a proglacial stream food web. *Limnol Oceanogr* 60:1118–1128
- Ge Q, Zheng J, Hao Z, Liu H (2013) General characteristics of climate changes during the past 2000 years in China. *Sci China Earth Sci* 56:321–329
- Guo LD, Ping CL, Macdonald RW (2007) Mobilization pathways of organic carbon from permafrost to arctic rivers in a changing climate. *Geophys Res Lett* 34:L13603
- Hågvar S, Ohlson M (2013) Ancient carbon from a melting glacier gives high ¹⁴C age in living pioneer invertebrates. *Sci Rep* 3:2820
- Holtvoeth J, Rushworth D, Imeri A, Cara M, Vogel H, Wagner T, Wolff GA (2016) Improved end-member characterization of modern organic matter pools in the Ohrid Basin (Albania, Macedonia) and evaluation of new palaeoenvironmental proxies. *Biogeosciences* 13:795–816
- Hood E, Battin TJ, Fellman JB, O’Neil S, Spencer RGM (2015) Storage and release of organic carbon from glaciers and ice sheets. *Nat Geosci* 8:91–96
- Hu Z, Anderson NJ, Yang X, McGowan S (2014) Catchment-mediated atmospheric nitrogen deposition drives ecological change in two alpine lakes in SE Tibet. *Glob Change Biol* 20:1614–1628
- Jeppesen E, Jensen JP, Skovgaard H, Hvidt CB (2001) Changes in the abundance of planktivorous fish in Lake Skanderborg during the past two centuries—a palaeoecological approach. *Palaeogeogr Palaeoclimatol Palaeoecol* 172:143–152
- Jeppesen E, Nöges P, Davidson TA, Haberman J, Nöges T, Blank K, Lauridsen TL, Søndergaard M, Sayer C, Laugaste R, Johansson LS, Bjerring R, Amsinck SL (2011) Zooplankton as indicators in lakes—a plea for including zooplankton in the ecological quality assessment of lakes according to the European Water Framework Directive (WFD)—*Hydrobiologia* 676: 270–297
- Jeziorski A, Paterson AM, Smol JP (2012) Changes since the onset of acid deposition among calcium-sensitive cladoceran taxa within soft water lakes of Ontario, Canada. *J Paleolimnol* 48:323–327
- Jiang XZ, Du NS (1979) *Fauna Sinica, crustacean: freshwater Cladocera*. Science Press, Beijing
- Kendrick MR, Hurn AD, Bowden WB, Deegan LA, Findlay RH, Hershey AE, Peterson BJ, Beneš JP, Schuett EB (2018) Linking permafrost thaw to shifting biogeochemistry and food web resources in an arctic river. *Glob Change Biol* 24:5738–5750
- Kong LY (2015) Study on the response of cladoceran in alpine lakes to environment change during the past 200 years in Western Sichuan Plateau. Dissertation. Nanjing Institute of Geography and Limnology
- Kong LY, Yang XD, Kattel G, Anderson NJ, Hu Z (2017) The response of Cladocerans to recent environmental forcing in an Alpine Lake on the SE Tibetan Plateau. *Hydrobiologia* 784:171–185
- Kuang XY, Liu J, Wang HL, Wang SM (2008) Interhemispheric comparison of climate change in the last millennium based on the ECHO-G simulation. *Chin Sci Bull* 53:2692–2700
- Legutke S, Voss R (1999) The Hamburg Atmosphere-Ocean Coupled Circulation Model ECHO-G. Technical Report No.18. Hamburg: German Climate Computer Center (DKRZ)
- Li ZG (2014) Glacier and Lake Changes across the Tibetan Plateau during the Past 50 years of climate change. *J Resour Ecol* 5:123–131
- Liu GM, Chen FZ, Liu ZW (2008) Preliminary study on cladoceran microfossils in the sediments of Lake Taihu. *J Lake Sci* 20:470–476
- Lotter AF, Birks HJB, Hofmann W, Marchetto A (1998) Modern diatom, cladocera, chironomid, and chrysophyte assemblages as quantitative indicators for the reconstruction of past environmental conditions in the Alps II. Nutrients *J Paleolimnol* 19:443–463
- Mahowald N, Jickells TD, Baker AR, Artaxo P, Benitez-Nelson CR, Bergametti G, Bond TC, Chen Y, Cohen DD, Herut B (2008) Global distribution of atmospheric phosphorus sources, concentrations and deposition rates, and anthropogenic impacts. *Glob Biogeochem Cycles* 22:37–42
- Manca M, Comoli P (2004) Reconstructing long-term changes in *Daphnia*’s body size from subfossil remains in sediments of a small lake in the Himalayas. *J Paleolimnol* 32:95–107
- Mayorga E, Aufdenkampe AK, Masiello CA, Krusche AV, Hedges JI, Quay PD (2005) Young organic matter as a source of carbon dioxide outgassing from Amazonian rivers. *Nature* 436:538–541
- Meyers PA, Teranes JL (2001) Sediment organic matter. In: Last WM, Smol JP (eds) *Tracking environmental change using lake sediments Terrestrial algal and siliceous indicators*, vol 3. Kluwer Academic Publishers, Dordrecht, pp 239–270
- Middelburg JJ (2014) Stable isotopes dissect aquatic food webs from the top to the bottom. *Biogeosciences* 11:2357–2371
- Mladenov N, Sommaruga R, Morales-Baquero R, Laurion I, Camarero L, Diéguez MC, Camacho A, Delgado A, Torres O, Chen Z, Felip M, Reche I (2011) Dust inputs and bacteria influence dissolved organic matter in clear alpine lakes. *Nat Commun* 2:405

- Nova CC, Bozelli RL, Spitz A, Müller-Navarra D (2019) Living in a browning environment: effects on *Daphnia*'s growth and fatty acid pattern. *Limnol Oceanogr* 64:18–31
- Orland IJ, Edwards RL, Cheng H, Kozdon R, Cross M, Valley JW (2015) Direct measurements of deglacial monsoon strength in a Chinese stalagmite. *Geology* 43:555–558
- Phillips DL, Gregg JW (2003) Source partitioning using stable isotopes: coping with too many sources. *Oecologia* 136:261–269
- Qiu J (2010) Measuring the meltdown. *Nature* 468:141–142
- Reimer PJ, Baillie MGL, Bard E, Bayliss A, Beck JW, Blackwell PG, Buck CE, Burr GS, Edwards RL (2013) IntCal13 and Marine13 radiocarbon age calibration curves 0–50,000 years cal BP. *Radiocarbon* 55:1869–1887
- Saros JE, Anderson NJ (2015) The ecology of the planktonic diatom *Cyclotella* and its implications for global environmental change studies. *Biol Rev Camb Philos Soc* 90:522–541
- Sichuan Statistical Yearbook (2005) Area ploughed by tractors and irrigated, consumption of chemical fertilizers, number of hydropower stations and electricity consumption in rural areas. Sichuan Provincial Bureau of Statistics
- Smol JP (2008) Pollution of lakes and rivers: a paleoenvironmental perspective. Blackwell Publishing, Oxford
- Søndergaard M, Liboriussen L, Asger R, Jeppesen E (2008) Lake restoration by fish removal: short- and long-term effects in 36 Danish lakes. *Ecosystems* 11:1291–1305
- Stibal M, Tranter M, Benning LG, Rehak J (2008) Microbial primary production on an Arctic glacier is insignificant in comparison with allochthonous organic carbon input. *Environ Microbiol* 10:2172–2178
- Stocker TF, Qin D, Plattner GK, Tignor M, Allen SK, Boschung J, Nauels A, Xia Y, Bex V, Midgley PM (2013) IPCC climate change 2013: the physical science basis. Cambridge University Press, Cambridge
- Sun HL (1996) Formation and evolution of Qinghai-Xizang Plateau. Shanghai Science Technology Press, Shanghai
- Szeroczyńska K, Sarmaja-Korjonen K (2007) Atlas of Subfossil Cladoceran from Central and Northern Europe. Friends of the Lower Vistula Society, Świecie, pp 10–11
- Taipale SJ, Brett MT, Hahn HW, Martin-Creuzburg D, Yeung S, Hiltunen M, Strandberg U, Kankaala P (2014) Differing *Daphnia magna* assimilation efficiencies for terrestrial, bacterial, and algal carbon and fatty acids. *Ecology* 95:563–576
- Tan LC, Cai Y, Cheng H, Edwards LR, Lan J, Zhang H, Dong L, Le M, Zhao P, Gao Y (2018) High resolution monsoon precipitation changes on southeastern Tibetan Plateau over the past 2300 years. *Quat Sci Rev* 195:122–132
- Thompson LG, Yao T, Mosley-Thompson E, Davis ME, Henderson KA, Lin PN (2000) A high-resolution millennial record of the South Asian monsoon from Himalayan ice cores. *Science* 289:1916–1919
- Vadeboncoeur Y, Jeppesen E, Zanden VMJ, Schierup HH, Christoffersen K, Lodge D (2003) From Greenland to green lakes: cultural eutrophication and the loss of benthic pathways. *Limnol Oceanogr* 48:1408–1418
- Wang Q, Anderson NJ, Yang X, Xu M (2020) Interactions between climate change and early agriculture in SW China and their effect on lake ecosystem functioning at centennial timescales over the last 2000 years. *Quat Sci Rev* 233:106238
- Wang R, Balkanski Y, Boucher O, Ciais P, Peñuelas J, Tao S (2015) Significant contribution of combustion-related emissions to the atmospheric phosphorus budget. *Nat Geosci* 8:48–54
- Wolff JO, Maier-Reimer E, Legutke S (1997) The Hamburg Ocean Primitive Equation Model. German Climate Computer Center (DKRZ) Technical Report No. 13, 98
- Xiao XY, Haberle SG, Shen J, Yang XD, Han Y, Zhang EL, Wang SM (2014) Latest Pleistocene and Holocene vegetation and climate history inferred from an alpine lacustrine record, northwestern Yunnan Province, southwestern China. *Quat Sci Rev* 86:35–48
- Yao TD, Wu GJ, Pu JC, Jiao KQ, Huang CL (2004) Relationship between calcium and atmospheric dust recorded in Guliya ice core. *Sci Bull* 49:706–710
- Zhang Y, Song L, Liu XJ, Li WQ, Lu SH, Zheng LX, Bai ZC, Cai GY, Zhang FS (2012) Atmospheric organic nitrogen deposition in China. *Atmos Environ* 46:195–204
- Zheng X, Fu C, Xu X, Yan X, Huang Y, Han S, Hu F, Chen G (2002) The Asian nitrogen cycle case study. *AMBIO A J Hum Environ* 31:79–87
- Zigah PK, Minor EC, McNichol AP, Xu L, Werne JP (2017) Constraining the sources and cycling of dissolved organic carbon in a large oligotrophic lake using radiocarbon analyses. *Geochim Cosmochim Acta* 208:102–108
- Zigah PK, Minor EC, Werne JP (2012) Radiocarbon and stable-isotope geochemistry of organic and inorganic carbon in Lake Superior. *Global Biogeochem Cycles* 26:1–20
- Zigah PK, Minor EC, Werne JP, McCallister SL (2011) Radiocarbon and stable carbon isotopic insights into provenance and cycling of carbon in Lake Superior. *Limnol Oceanogr* 56:867–886

Publisher's Note Springer Nature remains neutral with regard to jurisdictional claims in published maps and institutional affiliations.